Novel Class of Bivalent Glutathione *S*-Transferase Inhibitors†

Robert P. Lyon,‡ John J. Hill,§ and William M. Atkins*,‡

Department of Medicinal Chemistry, Box 357610, University of Washington, Seattle, Washington 98195-7610, and ICOS Corporation, Bothell, Washington 98021

Received April 18, 2003; Revised Manuscript Received July 15, 2003

ABSTRACT: Exploiting the principle of bivalent binding, we have designed symmetrical, bifunctional inhibitors to simultaneously occupy both active sites of cytosolic glutathione *S*-transferase, with enhanced specificity for the P1-1 isoform. We have prepared two series of compounds that differ in their binding domains—the first is a series of bis-glutathione conjugates, and the second is a series of compounds each possessing two equivalents of Uniblue A, an analogue of Cibacron Blue. For each series, a monofunctional reference compound was also prepared to determine the relative advantage of the bivalent inhibitors. Within each series, the most potent inhibitors exhibited IC_{50} values 2 orders of magnitude lower than the relevant reference compounds. Moreover, within the bis-glutathionyl series, a 10-fold increase in selectivity was achieved for GST P1-1 over the A1-1 isoform. Isothermal titration calorimetry with a representative bis-glutathione conjugate and a monofunctional reference compound indicates that the bivalent inhibitor exhibits the expected increase in intrinsic affinity and decrease in stoichiometry relative to the monofunctional compound, supporting the overall design strategy.

The glutathione *S*-transferases (GSTs)[1] are a family of cytosolic proteins with multiple known functions (*1*). The family takes its name from their most well-documented function, the catalytic activity wherein the nucleophilic tripeptide glutathione (GSH, γ-Glu-Cys-Gly) is conjugated to structurally diverse hydrophobic electrophiles. Among the electrophilic substrates for GSTs are alkylating agents used in the cytotoxic chemotherapy of many cancers, making this enzyme class of clinical relevance to oncologists. GSTs are known to be overexpressed in malignant tissues suggesting that they may play a role in acquired resistance to antitumor agents (*2*−*5*). Therefore, the coadministration of potent, selective GST inhibitors as adjuvants to cytotoxic chemotherapy has emerged as a possible strategy to restore the drug sensitivity of resistant cells. Moreover, it has recently been discovered that GST P1-1 may play a role in cell proliferation pathways via an interaction with Jun kinase, thus heightening interest in this isoform as a target for therapeutic intervention (*6*, *7*).

Toward this end, many groups have been pursuing the development of GST inhibitors for more than a decade (*8*−*10*). The currently existing GST inhibitors tend to fall into three classes, determined by their binding site on the protein and mechanism of inhibition. The first of these are analogues of electrophilic substrates, which bind in the hydrophobic region of the active site (H-site) and competitively inhibit the binding of hydrophobic electrophiles. Second are glutathione conjugates, which occupy both the glutathione binding site (G-site) and at least part of the H-site, and are typically competitive with respect to both glutathione and hydrophobic substrate. Third, a collection of compounds referred to as nonsubstrate ligands are noncompetitive inhibitors of the GSTs. These inhibitors are typically hydrophobic anions and include endogenous compounds such as porphyrins and bile acids and such exogenous compounds as sulfated organic dyes. The binding site of this group of inhibitors has historically been called the ligandin site, and its location remains uncertain; however, it may lie at one edge of the H-site or within the wide cleft between the two subunits of the GST dimer. These nonsubstrate ligands are unique among the GST inhibitors in that they elicit noncompetitive inhibition with respect to both glutathione and electrophilic substrate.

A common feature of these existing inhibitors is relatively low affinity, typically with K_i values in the μM range and with the very best compounds exhibiting K_i values on the order of 100 nM. Furthermore, many of these compounds inhibit multiple GST isoforms with little selectivity. Consequently, GST inhibitors with greater affinity and selectivity, particularly for GST P1-1, are necessary to further validate the concept of GST inhibition as a means of restoring sensitivity to drug resistant malignancies. For this reason, we prepared a novel class of GST inhibitors designed to exhibit both greater affinity and selectivity for GST P1-1.

The approach that we took in our inhibitor design is based on the concept of polyvalency, which has recently been applied to many biochemical systems to achieve considerable increases in both affinity and selectivity (*11*). Briefly, the underlying principle of the approach is that by incorporating

† This work was supported by National Institutes of Health Pharmacological Sciences Training Grant T32 GM07750 (R.P.L.), National Institutes of Health Grant GM62284, and the Department of Medicinal Chemistry, University of Washington.

* To whom correspondence should be addressed. Phone: (206) 685-0379. Fax: (206) 685-3252. E-mail: winky@u.washington.edu.

‡ University of Washington.

§ ICOS Corporation.

[1] Abbreviations: GST, glutathione *S*-transferase; GSH, reduced glutathione; CDNB, chlorodinitrobenzene; ITC, isothermal calorimetry; GS-DNB, glutathione-2,4-dinitrobenzene; CNBC, 4-chloro-3-nitrobenzoyl chloride.

10.1021/bi0346188 CCC: $25.00
Published on Web 08/15/2003

multiple binding domains within a single molecule, great improvements in affinity can be achieved due to the additivity of enthalpic binding terms without the additional entropic price of the loss of translational and rotational degrees of freedom associated with binding multiple individual molecules. Furthermore, because dramatic increases in affinity are only achieved if the geometry of the polyvalent molecule is appropriate for presenting each binding domain to a proper binding site, very high selectivity can also be attained. Many examples of polyvalent ligands have been reported, and their designs vary widely. One design employs symmetrical compounds that bind to symmetrical, multi-subunit proteins in which each binding domain occupies an equivalent binding site (*12*, *13*). A symmetrical compound has also been demonstrated to occupy asymmetrical binding sites of acetylcholinesterase with high affinity and selectivity (*14*). Another common approach employs asymmetrical bivalent ligands designed to bind at the cofactor and substrate sites of an enzyme, thus eliciting competitive inhibition (*15*). With respect to GST, the glutathione conjugates that have been widely used as inhibitors could be considered to fall into this latter category, with the glutathione moiety binding at the cofactor G-site and a hydrophobic moiety (ethacrynic acid, alkyl chain, etc.) binding at the substrate H-site. However, we observed that the geometry of the GST dimer, with its two identical active sites at opposite ends of a solvent-accessible intersubunit cleft, presents an opportunity to design novel bivalent inhibitors that occupy both active sites simultaneously (that is, both G-sites and/or both H-sites of the GST dimer). These compounds differ from other bivalent enzyme inhibitors described in the literature in that they bind to a symmetrical, dimeric enzyme possessing two equivalent active sites in close proximity (about 20 Å apart). Since each active site contains a glutathione binding subsite and a hydrophobic subsite, the binding domains of these inhibitors can be designed to occupy either or both of these subsites and thus be expected to exhibit competitive or noncompetitive inhibition kinetics with respect to GSH and electrophilic substrates. We present here the design and synthesis of two classes of symmetrical, bifunctional compounds and their kinetic characterization as inhibitors of GST isoforms P1-1 and A1-1.

EXPERIMENTAL PROCEDURES

Materials. Reduced glutathione was purchased from Sigma. The cross-linking agents ethylenediol bis-ethylamine and tetraethyleneglycol bis-amine were purchased from Molecular Biosciences. *N*-Boc-1,3-diaminopropane was purchased from Fluka. All other small molecule starting materials were purchased from Aldrich.

Recombinant human glutathione *S*-transferase A1-1 was expressed in *Escherichia coli* and purified as described previously (*16*). The enzyme was incubated with 10 mM dithiothreitol to ensure complete reduction of cysteine residues, followed by extensive dialysis to remove the reducing agent. Recombinant human glutathione *S*-transferase P1-1 was expressed and purified by the same protocol.

GST Kinetics. Assays of GST activity and inhibition were performed with chloro-2,4-dinitrobenzene (CDNB) as the electrophilic substrate. Except where otherwise stated, the GST concentration was 20 nM. For IC_{50} determinations, the concentration of GSH and CDNB were at their respective K_m values for each enzyme: 250 μM GSH for both enzymes, 750 μM CDNB for GST A-1, and 1.5 mM CDNB for GST P1-1. Rates were determined by measuring the absorption at 340 nm (λ_{max} of glutathione-dinitrobenzene) for 1 min on a Cary 3 spectrophotometer.

For IC_{50} determinations, assays were performed at inhibitor concentrations ranging over at least 5 orders of magnitude (from 100-fold above the IC_{50} to 100-fold below). Data were fit to the variable slope sigmoidal dose−response equation

$$v = \frac{100}{1 + 10^{B(\log IC_{50} - [I])}}$$

(where B is a factor that varies the slope of the curve to achieve the best fit) using GraphPad Prism to determine the 50% inhibitory concentration.

For variable substrate concentration assays with the bis-Uniblue A compound **7**, five CDNB concentrations (250 μM, 500 μM, 1 mM, 1.5 mM, and 2 mM) were paired with 3 mM GSH at five inhibitor concentrations (0, 25, 50, 100, and 200 nM). Data from these assays were fit to the equation

$$v = \frac{V_{max}[S]}{K_m\left(1 + \frac{[I]}{K_i}\right) + [S]\left(1 + \frac{[I]}{\alpha K_i}\right)}$$

by global nonlinear regression using Microcal Origin. As described previously (*17*), this equation is noncommittal with respect to the inhibition mechanism, and the convergence value of α provides a quantitative measure of the degree of competitiveness of the inhibition.

For variable enzyme concentration assays under inhibitor−depletion conditions with compound **6**, we performed assays at three GST P1-1 concentrations (5, 15, and 40 nM), matched with 12 inhibitor concentrations (2.5 nM, 5 nM, 10 nM, 25 nM, 50 nM, 100 nM, 250 nM, 500 nM, 1 μM, 2.5 μM, 5 μM, and 10 μM) at a CDNB concentration of 1.5 mM and a GSH concentration of 3 mM. Again, using global nonlinear fitting with Microcal Origin the results were fit to the equation

$$v_i = v_o \frac{[E] - [I] - K_i + \sqrt{([E] - [I] - K_i)^2 + 4[E]K_i}}{2[E]}$$

which describes the reaction rate in the presence of inhibitor (v_i) as the product of the uninhibited reaction rate (v_o) and the fraction of free enzyme (*18*, *19*). The quadratic term in the equation is derived from the expression of the inhibitor binding equilibrium, and the inhibitor concentrations are stated as total [I] rather than free [I] as in equations based on Michaelis−Menten kinetics. Note that the substrate concentration is not a variable in this equation, but enzyme concentration is.

Calorimetry. Isothermal titration calorimetry (ITC) measurements were carried out using a VP-ITC microcalorimeter (Microcal, Inc., Northhampton, MA) following standard instrumental procedures. The enzyme was dialyzed overnight at 4 °C in PBS buffer. Phosphate buffer was chosen by virtue of its small ionization enthalpy change; hence, the binding enthalpies reported for the protein−ligand interaction do not reflect a contribution due to buffer protonation. The enzyme

solution (~11 μM dimer) was in the calorimetric cell and titrated with ligand dissolved in the dialysate buffer at a concentration of ~ 600 μM. The actual protein concentrations for the replicate titrations were determined from absorbance measurements at 280 nm using ϵ_{280} 37 220 cm^{-1} M^{-1} as the molar extinction coefficient for the dimer, which was estimated from the protein primary sequence by Sednterp (V1.02) for Windows 95 and Windows NT (Created by David Hayes, Tom Laue, and John Philo), according to a method by Pace et al. (*20*). This free-ware program was obtained from the Reversible Associations in Structural and Molecular Biology (RASMB) software archive at http://www.bbri.org/rasmb/rasmb.html. Ligand samples were prepared from powder stocks by adding an appropriate aliquot of material into the dialysis buffer and shaking for 2 h. The undissolved ligand was pelleted by centrifugation, and the supernatant was collected for the titrations. The concentration of dissolved ligand was determined by HPLC analysis, relative to a standard curve prepared from powder stocks dissolved in DMSO. All experiments were performed at 30 °C, with a 250 μL injection syringe. A typical binding experiment involved 25−30 injections varying between 5 and 15 μL aliquots of ligand solution into the titration cell with 400 rpm stirring. Heats of dilution were determined by titrating ligand into buffer and buffer into protein. However, the heats of protein dilution were considered insignificant, so only the ligand dilutions were used to correct the total heats of binding prior to data analysis. The integrated heat effects were analyzed by nonlinear regression methods using the standard Microcal ORIGIN software package. The experimental data fit well to a model for simple binding to a single class of sites, yielding estimates of the apparent number of binding sites (n) on the protein, the association binding constant (K (M^{-1})) and the enthalpy of binding (ΔH (kcal/mol)). The entropy (ΔS (cal/K/mol)) associated with each binding reaction was calculated from the standard expression: $\Delta G^\circ = -RT \ln K = \Delta H^\circ - T\Delta S^\circ$. Values and uncertainties for n, K, and ΔH are the weighted averages and weighted standard deviations from four titration runs, using the χ^2 values and errors recovered from the fits. Values and uncertainties for the rest of the parameters were determined from these weighted average values and the propagation of their errors. The uncertainties primarily reflect the random errors associated with collecting and analyzing the experimental data. The errors inherent in determining the protein and ligand concentrations were not included in the analysis. These errors are primarily systematic and stem from the accuracy of the estimated extinction coefficient for the protein and the accuracy in preparing the ligand standard used in the HPLC analysis. The uncertainty in the extinction coefficient value was estimated to be ~4% (*20*), which translates into an approximately equivalent percentage error in the recovered number of binding sites (n). The uncertainty in the ligand standard curve was estimated to be ~1% (microbalance and pipetting errors), which translates into an approximately equivalent percentage error in all recovered parameters.

Molecular Modeling. Modeling of protein structures, including the determination of geometrical arrangements within protein−ligand complexes and the manual docking of proposed synthetic targets, was performed using UCSF MidasPlus. All protein crystal structures were retrieved from the Brookhaven Protein Data Bank. Geometry optimization and conformational analysis of small molecules for use in modeling protein−ligand interactions was performed using Spartan SGI version 4.0.4a GL (Wavefunction, Inc., Irvine, CA).

Preparation of Inhibitors. Electrospray ionization mass spectra of all compounds were obtained with a Fisons VG Quattro II mass spectrometer fitted with a Z-spray ESI source. Purified compounds were analyzed by direct injection into the instrument.

Bis-glutathionyl Nitrophenyl Derivatives. This series of three compounds (plus the monofunctional reference compound) is based on esters of 4-chloro-3-nitrobenzoyl chloride (CNBC). The alcohols required for the esterification are diols that represent the linker of each compound and are thus different for each compound in the series. One of the diols, tetraethyleneglycol, is commercially available, as is the alcohol (ethanol) used to prepare the monofunctional reference compound; the other two are based on diesters of isophthalic acid that had to be prepared separately.

To prepare the isophthalate diesters, isophthaloyl chloride was esterified to ethylene glycol or 1,3-propanediol. Because of the two equivalent reactive groups of isophthaloyl chloride and the diols, large excesses of the diols were necessary to prevent the formation of a polymeric species. Ethylene glycol and 1,3-propanediol (4 mL, about 60 mmol) were placed in two separate predried vials. Isophthaloyl chloride (0.5 mmol, 101.5 mg) was placed in each of two separate predried vials and dissolved in 1 mL of dry, freshly distilled THF. Using a dry syringe, the isophthaloyl chloride solution was added dropwise to each diol with vigorous stirring. Stirring was continued for 12 h, at which time TLC (ethyl acetate development, UV−vis) indicated no remaining isophthaloyl chloride (the limiting reagent). Water (8 mL) was added to each reaction, and then the solutions were extracted with 10 mL of toluene. The toluene extract contained a highly nonpolar species observed by TLC but little of the major product. The aqueous solutions were then extracted with 10 mL of either ethyl acetate (ethylene glycol ester) or diethyl ether (1,3-propanediol ester) and repeated four times. The five extracts for each product were combined and washed sequentially with water and saturated sodium chloride and then dried with anhydrous magnesium sulfate and evaporated under vacuum. The bis-ethanolisophthalate evaporated to a white solid that was recrystallized from anhydrous diethyl ether; the bis-propanolisophthalate evaporated to a colorless oil.

To prepare the linkers, tetraethyleneglycol, bis-ethanol-isophthalate, and bis-propanolisophthalate were esterified to two equivalents of CNBC. Each of the diols plus ethanol for the monofunctional reference compound (0.25 mmol) were placed in predried vials and dissolved in 1 mL of dry, freshly distilled pyridine. Four portions of CNBC (1.5 mmol) were placed in separate predried vessels and dissolved in 1 mL of dry pyridine. The diol (or ethanol) solutions were added dropwise to the CNBC solutions with stirring, producing an exothermic reaction and an immediate precipitate of pyridine hydrochloride. After 30 min, TLC (ethyl acetate development, UV−vis, and iodine staining) indicated no remaining diols (the limiting reagents) in any of the reaction media. The precipitates were removed by filtration, leaving pale yellow solutions in each case. Ice water (10 mL) was

added to each solution, resulting in immediate clouding of the solutions. Centrifugation resulted in the formation of off-white solid pellets in the case of the ethyl ester (monofunctional reference) and bis-ethanolisophthalate diester; the other reactions (tetraethyleneglycol diester and bis-propanol-isophthalate diester) yielded pale yellow oils. The solid products were filtered, washed with water, and dried in vacuo. Addition of 95% ethanol to the tetraethyleneglycol diester oil resulted in the formation of a nearly white precipitate that was filtered, washed sequentially with water and ethanol, and dried in vacuo. However, the bis-propanol-isophthalate diester remained oily after being washed with water and 95% ethanol.

The final step in the preparation of this series of compounds was glutathione substitution of the aryl chlorides. The monofunctional CNB ethyl ester (0.5 mmol, 115 mg) was dissolved in 2 mL of ethanol. GSH (1 mmol, 307 mg) was dissolved in 2 mL of water plus 334 μL of 6 M NaOH (2 mmol NaOH). To this solution, 95% ethanol was added until a slight cloudiness appeared (total volume about 6 mL). The CNB ethyl ester solution was then added dropwise to the GSH solution and allowed to stir for 48 h, producing a yellow solution. Each of the bis-CNB bifunctional diesters (0.075 mmol) were dissolved in 1 mL of acetonitrile. In three separate vials, GSH (0.375 mmol) was dissolved in 1 mL of water plus 125 μL of 6 M NaOH (0.75 mmol NaOH), and then acetonitrile (2 mL) was added to this solution. The bis-CNB bifunctional diester solutions were then each added to one of the GSH solutions. These mixtures were stirred for 48 h, producing yellow solutions in each case. All four of the above reaction mixtures were then evaporated under a stream of dry air to a volume of about 1 mL of predominately aqueous solution. These were placed in an ice bath and acidified to pH 3 by dropwise addition of 1 M HCl, producing yellow precipitates. After standing for 30 min, these mixtures were centrifuged, and the supernatants were discarded. The solid precipitates were resuspended in dilute HCl, filtered, and washed sequentially with water, acetonitrile, and diethyl ether and then dried in vacuo.

Bis-Uniblue A Derivatives. This series of three compounds is based on a series of diamines conjugated to the α,β-unsaturated sulfone moiety of the commercially available dye Uniblue A; the monofunctional reference is the ethylamine conjugate of this dye. Two of the diamines, ethylenediol bis-ethylamine (EDBEA) and tetraethyleneglycol bis-amine (TEGBA), are commercially available; the third is a diamide of isophthalic acid that had to be prepared separately.

To prepare the isophthalamide, isophthaloyl chloride (0.1 mmol, 20.3 mg) was placed in a predried vial and dissolved in 3 mL of dry, freshly distilled THF. Neat *N*-Boc-1,3-diaminopropane (0.286 mmol, 50 μL) was added dropwise from a dry syringe, producing an immediate white precipitate. After stirring for 30 min, the precipitate was filtered, and the THF solution was evaporated under vacuum, leaving an oily residue. This oil was dissolved in 10 mL of ethyl acetate and extracted sequentially with 10 mL each of water, 5% $NaHCO_3$, water, dilute HCl, and saturated NaCl. The washed ethyl acetate was then dried with anhydrous magnesium sulfate and evaporated under vacuum, leaving a colorless oil. This oil was then dissolved in $CHCl_3$ (3 mL) and 300 μL of trifluoroacetic acid was added to effect cleavage of the Boc protecting group and yield the bis-propylamine-isophthalamide. After stirring for 30 min, TLC (alumina plate, methanol development, UV−vis) indicated that complete cleavage had been effected. The solution was then evaporated under vacuum to a colorless oil, which was washed with hexane and dried in vacuo.

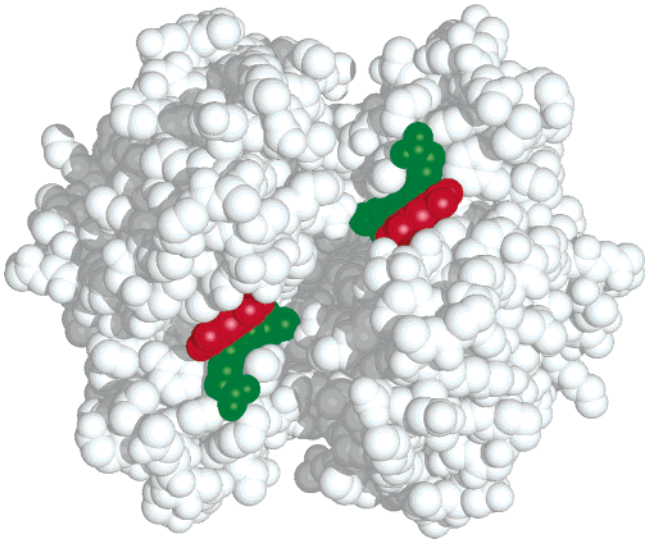

FIGURE 1: Space-filling model of the complex of GST P1-1 and GS-DNB, illustrating the solvent-accessible intersubunit cleft. Glutathione moieties are shown in green, dinitrophenyl moieties in red.

Conjugation of the diamines with Uniblue A was effected by dissolving each diamine (0.1 mmol) in 1 mL of water, then adding this to a solution of Uniblue A (0.3 mmol) in 4 mL of water. The pH of these solutions was found to be about 10.5 for the EDBEA and TEGBA solutions but about 2.0 for the bis-propylamineisophthalamide. The pH of this solution was raised to 10.5 with saturated Na_2CO_3. The solutions were stirred for 2 days, and the bis-Uniblue A products were purified from the reaction medium by preparative HPLC. The products were the final species to elute from a 10 mm i.d. C_{18} column eluted with 30% acetonitrile/70% water. For each product, the pooled dark blue fractions were evaporated under a stream of air; as the acetonitrile was removed, a dark blue precipitate was formed. When little color remained in solution, the precipitate was filtered and dried in vacuo. Conjugation of Uniblue A with ethylamine to prepare the monofunctional reference compound was performed similarly to the above procedure, but 0.1 mmol of Uniblue A (50 mg) was mixed with 0.1 mmol of ethylamine (6.5 μL of a 70% aqueous solution). HPLC purification was performed as above.

RESULTS

We used the structure of GST P1-1 as the basis for designing bivalent inhibitors to maximize selectivity for this isoform. The crystal structure of GST P1-1 in complex with glutathione-2,4-dinitrobenzene (GS-DNB) shown in Figure 1 (PDB entry 18GS) illustrates the location of the H- and G-sites of each monomer and the positions of the two active sites relative to each other (*21*). These active sites are positioned at the ends of the deep, solvent-accessible cleft that lies above the subunit interface. Because of the proximity of the two active sites of the GST dimer and their location at opposite ends of the solvent-accessible intersubunit cleft,

we reasoned that bifunctional inhibitors could be designed to simultaneously occupy both active sites. The binding domains of such a molecule require a linker that can bridge and thus partially occupy the intersubunit cleft. Given that this cleft is postulated to be a ligand binding site and two crystal structures of different GST isoforms have been reported with ligands bound within the cleft, it seems reasonable that a linker could occupy this region without inducing significant changes in the protein architecture.

The design considerations of bifunctional inhibitors can be divided into two elements: the binding domains and the molecular linker between them. We have designed two classes of inhibitors that differ in their binding domains. These two classes of compounds and the molecular linkers used for each will be presented separately.

Bis-glutathionyl Nitrophenyl Derivatives. Design. A close examination of the crystal structure of the complex between GST P1-1 and GS-DNB (Figure 1) suggested that *S*-phenyl glutathione conjugates may be ideal in their ability to anchor the binding moiety in an appropriate orientation for bivalent binding in the manner that we have envisioned. Within the H-site of P1-1, the phenyl moiety of the GS-DNB ligand is stacked with the side chain of tyrosine 108. This aromatic interaction, which does not exist in A1-1 because of the exclusively aliphatic residues along the side of the H-site of that isoform, orients the ring such that the para-nitro group is pointed toward the intersubunit cleft, and its counterpart is bound to the other subunit. We hypothesized that this interaction may therefore produce a solid anchorage of the two binding domains of a bifunctional inhibitor of GST P1-1. The para-carbon of this ring seemed a reasonable attachment point for a linker that would join two analogues of GS-DNB. The distance between the para-carbons of the two GS-DNB moieties observed in the P1-1 crystal structure is 19.2 Å.

To prepare bifunctional analogues of GS-DNB, we selected 4-chloro-3-nitrobenzoyl chloride (CNBC) as a precursor. This reagent presents a reactive acyl halide in place of the para-nitro group and is thus easily cross-linked at this position. However, it retains the highly electron withdrawing nitro group ortho to the chloro substituent, thus retaining the reactivity at this site (for ensuing substitution with glutathione) and the electron deficient nature of the aromatic ring in the final product.

Preparation. We employed linkers of varying lengths to bracket the spacing observed in the crystal structure. We also employed linkers with varying degrees of internal flexibility, from fully rotatable poly(ethylene glycol) (PEG) polymers to aromatic diesters of isophthalic acid. As described in the Experimental Procedures, each of these cross-linkers was esterified to two equivalents of CNBC, followed by conjugation with two equivalents of glutathione to create the set of compounds (**2**−**4**) illustrated in Figure 2. The length of the resulting compounds (between the para-carbons) when modeled in an extended conformation is also shown in Figure 2. As a monofunctional benchmark to assess the relative advantage of bifunctionality, the ethyl ester of CNBC was also prepared, then conjugated with one equivalent of glutathione (Figure 2, compound **1**).

Kinetics. The concentration required for 50% inhibition (IC_{50}) of GST isoforms P1-1 and A1-1 was determined for compounds **1**−**4** using the CDNB assay; these data are

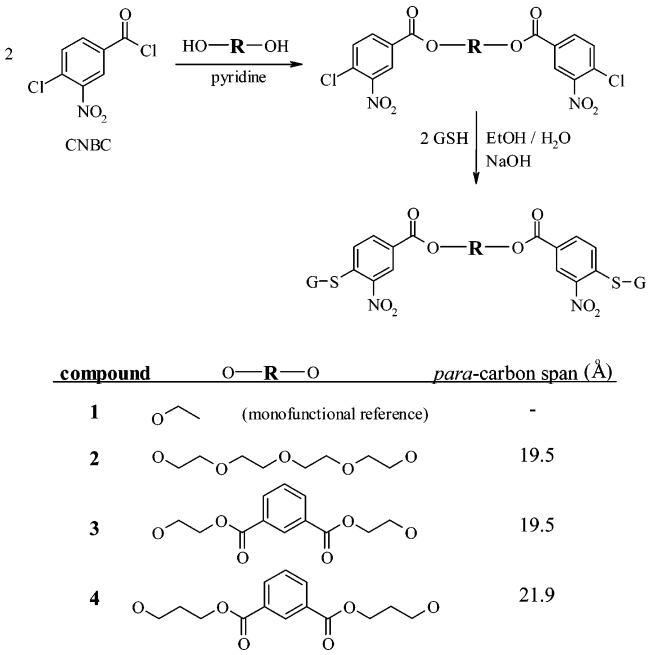

FIGURE 2: Scheme for the preparation of a series of bis-glutathionyl nitrophenyl derivatives. Compound **1** is the monofunctional reference prepared by the esterification of ethanol with only 1 equiv of CNBC.

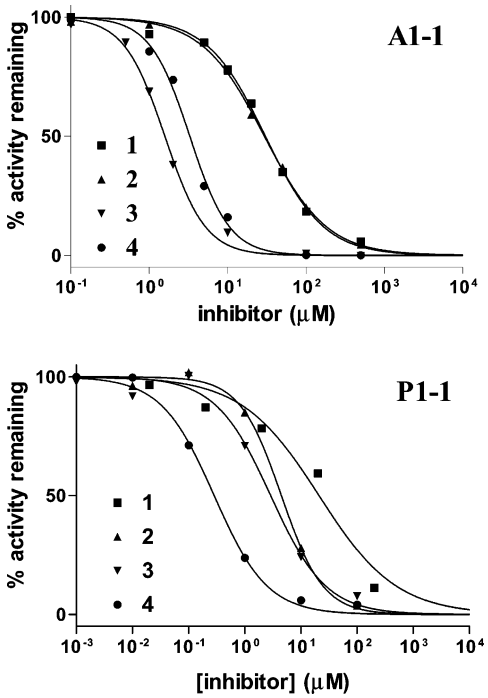

FIGURE 3: Inhibition of GST A1-1 and P1-1 by bis-glutathionyl nitrophenyl derivatives. See Figure 2 for structures of compounds **1**−**4**. Numerical IC_{50} values are tabulated in Table 1.

plotted in Figure 3. The resulting IC_{50} values are tabulated in Table 1 along with the observed slopes of the inhibition curves. Interestingly, those bifunctional compounds that exhibit significantly higher affinity than the monofunctional reference compound **1** also exhibit significantly steeper slopes of their inhibition curves. Although the IC_{50} experiment does not yield information about the inhibition mechanism, these compounds are almost certainly competitive with respect to both GSH and CDNB. These assays were performed with concentrations of GSH and CDNB equal to

Table 1: IC_{50} Values of Bis-Glutathionyl Nitrophenyl Derivatives with GST A1-1 and P1-1 and the Slopes (with Standard Errors) of the Inhibition Plots; Values Are Derived from the Plots Shown in Figure 3

	A1-1		P1-1	
compound	IC_{50} (μM)	slope (B)	IC_{50} (μM)	slope (B)
1	30	−1.17 (0.06)	21	−0.63 (0.12)
2	29	−1.09 (0.03)	4.5	−1.17 (0.11)
3	1.6	−1.67 (0.13)	2.9	−0.88 (0.11)
4	3.3	−1.71 (0.11)	0.28	−0.92 (0.07)

Table 2: Experimental Thermodynamic Data for Glutathionyl Nitrophenyl Ligands Binding to GST, Determined by ITC at 30 °C[a]

parameter	monofunctional (**1**)	bivalent (**3**)
K_d (μM)	8.5 ± 0.3	0.58 ± 0.02
n (stoichiometry)	1.98 ± 0.02	1.24 ± 0.005
ΔH (kcal/mol)	−9.3 ± 0.1	−21.1 ± 0.1
ΔS (cal/mol K)	−7.7 ± 0.4	−41.0 ± 0.4
ΔS_{ind} (cal/mol K)	+8.0 ± 0.4	−32.0 ± 0.4
ΔG (kcal/mol)	−7.01 ± 0.02	−8.63 ± 0.02

[a] ΔS_{ind} represents an entropic factor corrected for the entropy of mixing (see text).

their respective K_m values. Under these conditions, it can be seen that 25% of the enzyme population is bound with both substrates (as there is known to be no cooperativity between the two); thus, the K_i can be estimated as $IC_{50} = 4K_i$ for inhibitors that are competitive with both substrates, as these are expected to be. Note that this is a modification of the standard Cheng−Prusoff relationship $IC_{50} = 2K_i$ for standard competitive inhibitors with respect to a single substrate (*22*).

Calorimetry. ITC is a well-established method for the measurement of the stoichiometry (n), the dissociation constant (K_d), and the enthalpy and entropy (ΔH and ΔS, respectively) changes of a binding reaction and has previously been applied to measuring the thermodynamics of ligand binding to GST A1-1 (*23*). ITC experiments with GST A1-1 and the most potent bis-glutathionyl compound for this isoform (**3**) and the monofunctional reference compound (**1**) were carried out to determine the stoichiometry of binding and the intrinsic affinities of these two ligands for the enzyme. Typical experimental data, raw and fitted, are given in Figure 4a,b (monofunctional and bivalent ligands, respectively). The spike in the instrumental response that occurs halfway through the experiment corresponds to the switch to a larger injection volume. Analysis of the data yields a binding affinity (K_d) of 8.5 μM for the monofunctional ligand (**1**) and 0.58 μM for the bivalent ligand (**3**) (Table 2), which are very similar to the apparent inhibition constants (K_i) determined from the enzymatic assays of 7.5 and 0.4 μM, respectively (Table 1, where $K_i = 1/4IC_{50}$). Moreover, the stoichiometries of binding for the monofunctional ligand (**1**) and the bivalent ligand (**3**) of 1.98 and 1.24, respectively, are in strong agreement with the principle that the bivalent ligand is primarily binding to a single dimeric enzyme. The slightly greater value than unity for the bivalent stoichiometry may be due in part to other complexation species such as two separate bivalent ligands binding to a single GST dimer. It is unlikely that these other species could be resolved from the single bivalent−dimer interaction in the calorimetric trace. The binding enthalpy of **3** is 2-fold greater than that of **1**, consistent with the two binding domains of the bivalent ligand adopting a binding mode similar to that of the monovalent compound, with the linker not contributing significantly to ΔH. The entropic parameters are presented in Table 2 using two different standard state scales, to most accurately assess the entropic contribution of bivalency while also providing parameters that can be directly compared to others in the biophysical literature (*24*, *25*). The ΔG, ΔH, and ΔS values are referenced to a biochemist's standard state, defined as the changes in free energy, enthalpy, and entropy when all components are at 1 M, pH 7.4, 303 K. These values are obtained using molarity units in the calculation. This standard state, or one at a similar temperature, is used nearly universally for protein−ligand interactions, and it provides a convenient reference for comparing relative affinities and thermodynamic parameters across various proteins and ligands. On the basis of these values, the enthalpy contributes to the enhanced affinity of the bivalent ligand, but the entropy of the binding in dilute solution is extremely unfavorable. In fact, one may conclude that the entropy for the bivalent inhibitor is less favorable than the monovalent compound, in contrast to the theory concerning the thermodynamic origins of multivalency. However, the ΔS term is dependent on the choice of a standard state scale; hence, it may not accurately reflect the entropic handicap or advantage of the bivalent compound. This is because the entropic term consists of a cratic component that is composition-dependent and a composition-independent component. The composition-independent component is essentially the result of the entropy of mixing, which includes a statistical factor that differs for the case of two ligands binding to a protein (a three-body reaction) versus a single bivalent ligand binding to a protein (a two-body reaction). The enthalpy term is independent of the standard state scale. The composition-independent terms ΔS_{ind} can be approximated as

$$\Delta S_{ind} = \Delta S - \Delta qR \ln 55.5$$

where Δq is the change in molecularity of the reaction, or (number of product species) − (number of reactant species). The values are $\Delta q = -1$ and $\Delta q = -2$ for the bivalent and monovalent inhibitors, respectively. As pointed out by others (*26*), the sign of ΔS_{ind} may even be opposite to the corresponding signs of ΔS, as is the case here for the binding of the monovalent ligand.

An additional feature of the calorimetry data is the observation that the bifunctional ligand undergoes a large endothermic change upon dilution (inset, Figure 4b) suggesting that some intermolecular association present in the concentrated stock solution is disrupted upon dilution. The heat of dilution for the monofunctional ligand (not shown) was relatively low and exothermic.

bis-Uniblue A Derivatives. Design. A recently published crystal structure (PDB entry 20GS) of GST P1-1 in complex with Cibacron Blue was used as the basis for the second set of inhibitors. In this structure (Figure 5, top), only the anthraquinone sulfonate moiety was crystallographically observed, with no electron density seen for approximately half of the molecule (*27*). The anthraquinone sulfonate thus seems to be the binding determinate for the relatively high affinity interaction between Cibacron Blue and GST P1-1. We reasoned that an analogue of Cibacron Blue that contained this binding determinate but that possessed a

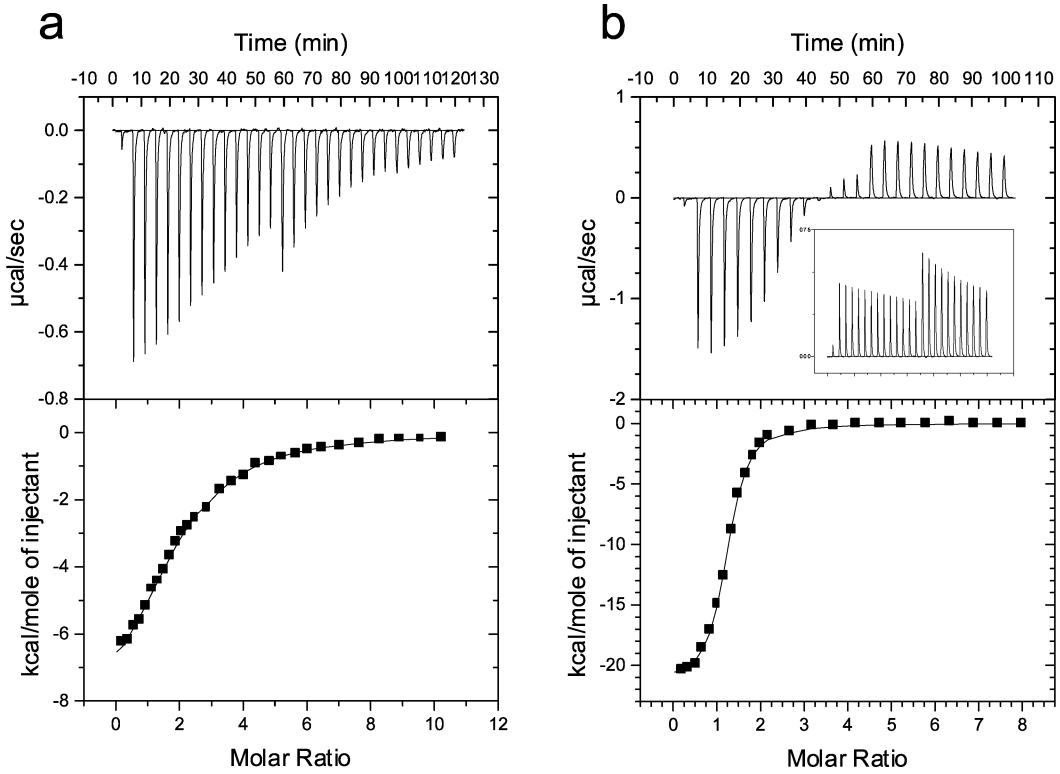

FIGURE 4: Calorimetric titration of GST A1-1 with the monofunctional ligand **1** (a) and bivalent ligand **3** (b) in PBS buffer at 30 °C. Top panels show the heat effects associated with the injection of ligand into the cell containing GST. Bottom panels show the binding isotherm, generated from the integrated heats in the top panel, and the best fitted curves (see text and tables for details). The inset in panel b shows the corresponding heat of dilution for the bivalent ligand into buffer.

reactive handle appropriately positioned for cross-linkage with a second moiety would be a good candidate for a bifunctional inhibitor. We therefore selected Uniblue A as the binding moiety, which possesses all of the structural elements observed in the Cibacron Blue−GST P1-1 complex and has a reactive α,β-unsaturated sulfone moiety for cross-linkage (Figure 5, bottom). When two molecules of Uniblue A are overlaid with the observable anthraquinone moieties of Cibacron Blue in the GST P1-1 complex, their reactive β-carbons are 16.2 Å apart. We again employed linkers to bracket this distance and to vary the degree of internal flexibility.

Preparation. As with the bis-glutathionyl nitrophenyl derivatives discussed above, we employed linkers with varying degrees of internal flexibility, including two poly(ethylene glycol) (PEG) polymers and an aromatic diamide of isophthalic acid. As described in the Experimental Procedures, these diamino linkers were conjugated to the α,β-unsaturated sulfone moieties of two equivalents of Uniblue A to prepare the bifunctional compounds **6**−**8** shown in Figure 6. The length of the resulting compounds (between the β-carbons) when modeled in an extended conformation is also shown in Figure 6. The monofunctional derivative **5** (Figure 6) was prepared with ethylamine to serve as a benchmark compound.

Kinetics. Again, the CDNB assay was employed to determine IC_{50} values for compounds **5**−**8** with GST isoforms P1-1 and A1-1. However, these compounds (including the monofunctional ethyl ester **5**) did not exhibit any inhibition of GST A1-1 at the highest inhibitor concentration tested (100 μM). The inhibition data for P1-1 are plotted in Figure 7. The resulting IC_{50} values are tabulated in Table 3 along with the observed slopes of the inhibition curves. As with the bis-glutathionyl nitrophenyl derivatives, the highest affinity compound (**6**) exhibits an IC_{50} approximately 2 orders of magnitude lower than that of the monofunctional reference compound, **5**. Interestingly, in this series of compounds, the two members with the flexible, ethylene glycol-based linkers both exhibit higher affinity than the isophthalamide-based compound, which is in contrast to the results seen in A1-1 inhibition by the bis-glutathionyl nitrophenyl derivatives. Again, the bifunctional compounds exhibit significantly higher affinity than the monofunctional reference compound **5** and also exhibit significantly steeper slopes of their inhibition curves.

Many nonsubstrate ligands such as Cibacron Blue have been reported to be noncompetitive inhibitors of the GSTs. Since the mechanism by which **5**−**8** elicit inhibition cannot be discerned from the IC_{50} determination, we selected the highest affinity compound of this series (**6**) and performed assays at variable CDNB concentrations to determine the K_i and inhibition mechanism as described in the Experimental Procedures. The results of this global nonlinear treatment of the inhibition data are shown in Figure 8. The convergence values for the fitting parameters, as shown in the figure, are an α value of 6 and a K_i of 50 nM. The α of 6 suggests that compound **6** is partially competitive with CDNB (i.e., a 6-fold increase in K_m upon binding of **6**) and is indicative of a mixed inhibition mechanism (*17*). The determined K_i is similar to the observed IC_{50} of 44 nM, suggesting that **6** is one of the highest affinity GST P1-1 inhibitors to have been reported.

However, these assays (and the IC_{50} assays) were conducted at a GST concentration of 20 nM, meaning that the

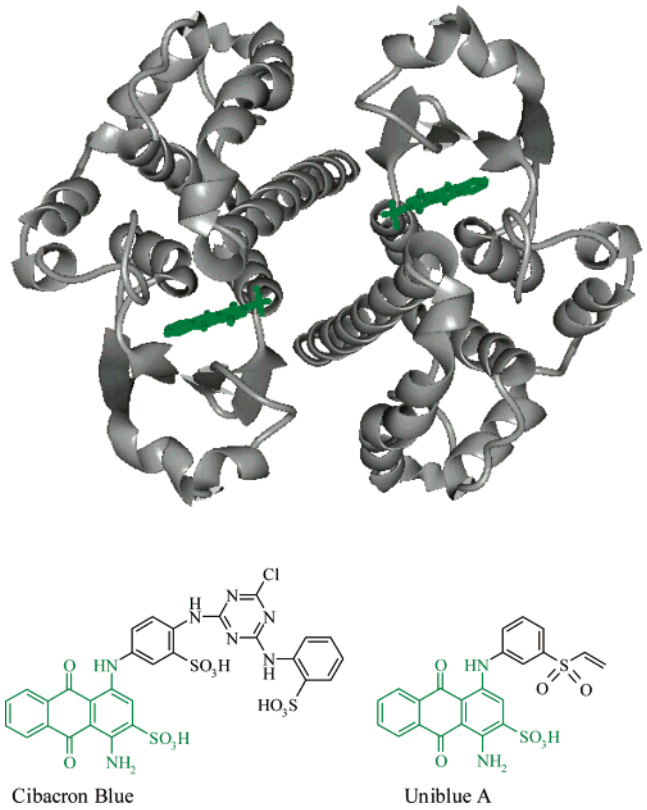

FIGURE 5: Top: ribbon diagram of the complex between GST P1-1 and Cibacron Blue; only the anthraquinone sulfonate moiety of the ligand is crystallographically observed (green). Bottom: structures of Cibacron Blue and Uniblue A. The anthraquinone sulfonate moiety of Cibacron Blue shown in green corresponds to that portion of the structure that is crystallographically observed in the P1-1 complex (top). This binding moiety is preserved in Uniblue A as shown on the right.

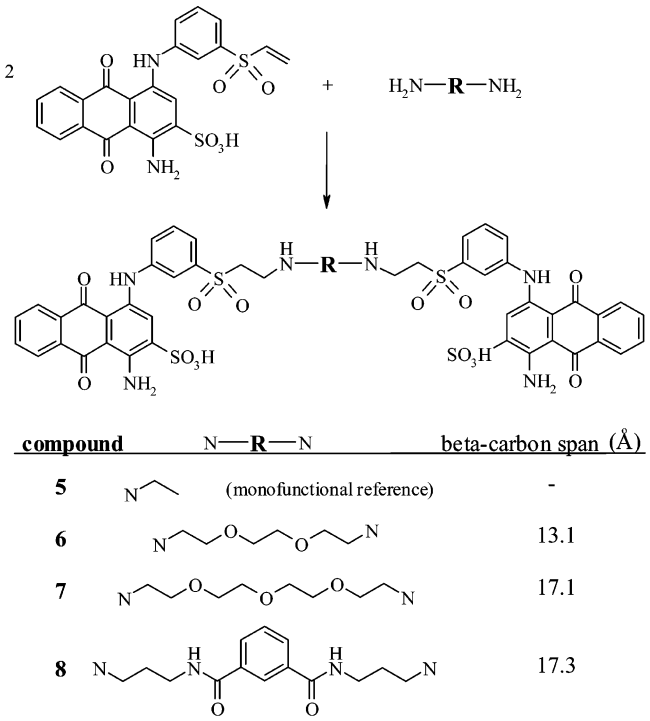

FIGURE 6: Scheme for the preparation of a series of bis-Uniblue A derivatives.

assays at the lowest inhibitor concentrations contained a concentration of **6** scarcely above that of GST. Under such

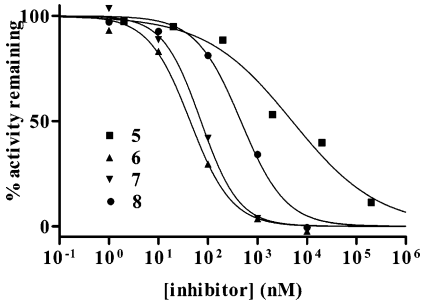

FIGURE 7: Inhibition of GST P1-1 by bis-Uniblue A derivatives. See Figure 6 for structures of compounds **5**−**8**. Numerical IC_{50} values are tabulated in Table 2.

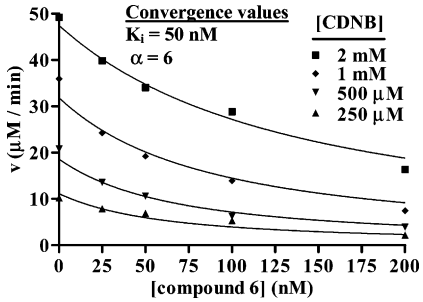

FIGURE 8: Global nonlinear fit of P1-1 inhibition data by compound **6**. The best fit values for K_i and α are 50 and 6 nM, respectively; see Experimental Procedures for the fitting equation.

Table 3: IC_{50} Values of Bis-Uniblue A Derivatives with GST P1-1 and the Slopes (with Standard Errors) of the Inhibition Plots[a]

	P1-1	
compound	IC_{50} (nM)	slope (B)
5	5000	−0.50 (0.06)
6	44	−1.03 (0.08)
7	72	−1.14 (0.16)
8	440	−0.87 (0.18)

[a] Values are derived from the plots shown in Figure 7.

inhibitor depletion conditions, the equations describing Michaelis−Menten kinetics do not neatly apply, as these assume that the total concentration of inhibitor (which is known) is equal to the concentration of free, unbound inhibitor (which is unknown). Compounds with such high affinity as to produce these conditions are often referred to as tight-binding inhibitors. Although some may not consider that a 50 nM K_i suggests a tight-binding inhibitor, from an experimental point of view the only relevant factor is the ratio of the values of K_i and the enzyme concentration that must be employed in the assay. To more accurately determine the inhibition constants of tight-binding inhibitors, a more complex treatment needs to be employed. As described in the Experimental Procedures, we performed assays at variable enzyme concentrations and fit the data to the appropriate quadratic equation. This analysis (not shown) yielded a K_i of 45 nM, only slightly lower than the value obtained from the Michaelis−Menten analysis. However, this method does not provide insight as to the inhibition mechanism, and the K_i that it produces is actually an apparent K_i, equal to the true K_i only in the case of noncompetitive inhibitors; for purely competitive inhibitors, the true K_i is derived by dividing the apparent K_i by the factor $1 + [S]/K_m$ (*28*). Because the previous analysis suggested mixed inhibition is operative in this case, it appears probable that the true K_i is

lower than the apparent K_i; however, regardless of this uncertainty the observed value of 45 nM may be considered an upper limit for the K_i of compound **6**. Since this compound did not exhibit inhibition of A1-1 at the concentrations tested, isozyme selectivity cannot be precisely quantified; however, selectivity of the bivalent compound for P1-1 over A1-1 is greater than 3 orders of magnitude given the P1-1 K_i of about 40 nM and zero A1-1 inhibition at 40 μM.

DISCUSSION

The goal of this study was to apply the principle of bivalency to GST P1-1 by developing bifunctional inhibitors that exhibit a significantly higher affinity and isoform selectivity than appropriate monofunctional analogues. Toward this end, we prepared several compounds based on the theme of two binding moieties separated by a spacer of appropriate length to place these moieties at the two active sites of a GST dimer. By varying the composition of these linkers, we sought optimal geometries for GST P1-1, thus attaining isoform selectivity while simultaneously improving affinity through bivalent binding.

The series of bis-glutathionyl nitrophenyl derivatives we prepared (**2**−**4**, Figure 2) appear to exhibit the characteristics expected of bivalent ligands, with inhibition kinetics highly sensitive to changes in the linker length and composition. For example, compounds **3** and **4**, which differ in length by only two methylene units, differ in their P1-1 IC_{50} values by an order of magnitude (Figure 2, Table 1). With GST A1-1, the bifunctional compound **2** exhibits no advantage over the monofunctional benchmark **1**, while the other two bifunctional compounds each exhibit an order of magnitude higher affinity. The importance of linker composition is illustrated by comparing compounds **2** and **3**—the linkers are of the same length, but the more rigid isophthaloyl linker yields an A1-1 IC_{50} value about 10-fold lower than the completely flexible tetraethyleneglycol linker. Indeed, the more rigid linkers (**3** and **4**) exhibit generally lower IC_{50} values for both enzymes than the flexible linker (**2**), perhaps due to a greater loss of conformational entropy upon binding a flexible moiety. For the P1-1 isoform, **4** is the highest affinity bifunctional compound, exhibiting an IC_{50} about 2 orders of magnitude lower than the monofunctional benchmark compound **1** and 10-fold selectivity for GST P1-1 over A1-1. These results validate the approach of bivalency as we have applied it to designing the inhibitors of GST as they demonstrate that the affinity and specificity of two identical binding moieties can be modulated by varying the length and chemical composition of the linker between them.

Compounds **6**−**8** (Figure 6) were designed to employ nonsubstrate ligands as the binding domains of a series of bifunctional inhibitors. Two of these compounds (**6** and **7**) again exhibit P1-1 IC_{50} values 2 orders of magnitude lower than the appropriate monofunctional reference compound **5** (Figure 7, Table 2). However, none of these compounds (including the monofunctional reference) exhibited inhibition of A1-1, so no statements can be made about how the bifunctional approach in this case affected isoform selectivity. However, it should be noted that compound **6**, with a K_i on the order of 45 nM, is the tightest-binding GST P1-1 inhibitor of which we are aware.

It is interesting to note that many of the compounds that exhibit significantly higher affinities than their respective monofunctional references also exhibit significantly steeper slopes in their inhibition curves. This is best exemplified by the inhibition data for the bis-glutathionyl nitrophenyl derivatives with A1-1 (Figure 3, top). In these data, the monofunctional reference (**1**) and the low affinity bifunctional inhibitor (**2**) exhibit a concentration span of about 1.8 log units between the 10 and the 90% inhibition levels, similar to the 1.9 log units expected of a ligand binding to a single site in the absence of cooperativity. In contrast, the two inhibitors (**3** and **4**) that exhibit IC_{50} values significantly lower than the monofunctional reference (**1**) possess very steep curves; the span of inhibitor concentrations between 10 and 90% inhibition is about 1.1 log units. These slopes are quantified by the *B* factors in the fitting equation (see Experimental Procedures). The high affinity bifunctional compounds **3** and **4** exhibit *B* factors about 1.5-fold higher than those of the lower affinity compounds (Table 1). Such increases in the slope of a binding curve are generally attributed to cooperativity. In this case, the concept of cooperativity does not precisely apply, as cooperative binding is generally considered to be induced by a change in the protein or receptor rather than in some property of the ligand. Nonetheless, one of the principles of cooperativity does apply to bivalent ligands—that the dissociation constant of the second binding moiety of a bivalent ligand is lower than that of the first, due in principle to the lower entropic cost of the second binding event. Since bivalent binding should inhibit twice as many active sites than a monovalent inhibitor per unit of concentration, it may not be unreasonable to expect the binding (or inhibition) curve of a bifunctional ligand to resemble cases of positive cooperativity. The situation is analogous to the curves obtained from the titration of a solution of metal ions with polydentate versus unidentate ligands. Analytical chemists have long known that polydentate ligands such as EDTA will yield much steeper titration curves (and sharper endpoints) than those obtained with a unidentate ligand such as acetate (*29*). We are unaware of variable slopes in inhibition curves being reported in the context of bivalent enzyme inhibitors, but we propose that this could be a generally observed phenomenon in cases where a single multivalent inhibitor occupies multiple enzyme active sites.

The ITC data clearly support the increased affinity of the bivalent inhibitors versus the monovalent analogues as observed in the inhibition experiments. In addition, they further demonstrate the difference in stoichiometry expected for monovalent versus bivalent interactions (1.2:1 vs 1.9:1), supporting the overall design strategy. The observed difference in ΔH between the two compounds is very close to the expected change for a bivalent inhibitor in which the linker does not interact significantly with the protein. That is, a ΔH value that is twice as large for the bivalent versus monovalent compound is expected, and this is observed. However, the entropic terms do not demonstrate the expected behavior. The apparent $\Delta\Delta S$ between monovalent and bivalent compounds is ~33 entropy units for the experimental data calculated with a standard state of 1 M, but this value increases to ~40 entropy units when the statistical entropy of mixing is accounted for. Thus, the apparent deviation from the theoretical entropic basis for the advantage of multivalency is even greater than the experimental values would indicate—binding of the bivalent compound carries a

greater entropic cost than binding of the monovalent compound. The monovalent compound must pay an entropic price for forfeiting translational and rotational motion, but presumably it displaces ordered water molecules that then gain these degrees of freedom, resulting in a small net entropic gain. The observed decrease in entropy upon binding of the bivalent compound likely arises from immobilization of the flexible linker, which contains 10 rotatable bonds. Presumably, restriction of rotational freedom within the linker upon binding offsets any entropic gain of limiting the translational entropy of the binding element in the bivalent compound. It thus appears that in this case, the basis for the improved affinity of the bivalent compound is its significantly more favorable binding enthalpy, which is partially offset by a less favorable binding entropy. It is notable that the improvement in affinity that we observe for the bivalent ligand (about 15-fold lower K_d) is indeed quite modest when compared to other engineered bivalent ligands with more rigid linkers (*11*−*15*). This provides an instructive example of the magnitude of the entropic penalty incurred by a flexible linker.

Regardless of the underlying thermodynamic basis in this particular case, the data clearly demonstrate a very significant increase in affinity for bivalent inhibitors of several structural classes, for two different GST isoforms. Exploration of optimal linker characteristics will almost certainly provide additional benefits. These analyses exemplify the difficulty in interpreting in molecular terms, and quantifying, the thermodynamic basis for increased affinity of multivalent inhibitors.

As an interesting aside, it is notable that the bivalent compound has such a dramatically different heat of dilution than the monovalent compound. This provides a clear reminder that inhibitor−solvent interactions contribute to the thermodynamics of binding, in addition to the well-appreciated protein−inhibitor (and protein−solvent) interactions, and the solvent interactions should be considered in design strategies. It will be interesting to perform additional calorimetric experiments with other bivalent−monovalent pairs to determine if this difference in the heat of solution is a generally observed phenomenon and whether the molecular basis of the effect can be determined.

The goal of designing GST inhibitors is eventually their use in cell- or animal-based models to assess their effectiveness in restoring alkylating agent sensitivity to resistant tumor cells, and ultimately as drugs in clinical use. It is clear that glutathione-based compounds would make poor drugs for several reasons. First, their ability to cross cellular membranes is likely very poor due to the highly charged and hydrophilic nature of glutathione. Second, even if they managed to diffuse into a cell, the presence of glutathione conjugate efflux pumps would result in the active transport of the compound out of the cell. Furthermore, they would likely be subject to rapid degradation by γ-Glu-Cys peptidase, the first enzyme in the mercapturic acid excretion pathway for glutathione conjugates. Finally, any glutathione conjugate inhibitor would almost certainly be competitive with respect to glutathione, which is present at intracellular concentrations greater than 20-fold above its K_m with GST. Therefore, to effectively compete (and thus inhibit the enzyme), an inhibitor would need to reach free, unbound intracellular concentrations at least 20-fold above its K_i; due to the difficulties stated above, this would appear to be very difficult to achieve. For all of these reasons, inhibitors based on binding domains that occupy the hydrophobic substrate site or the ligandin site would seem to have greater potential. Molecules similar in design to the bis-Uniblue A derivatives would therefore be ideal candidates for further study.

ACKNOWLEDGMENT

The authors would like to thank Michael Dabrowski for assistance with the preparation of the recombinant GSTs used in this work.

REFERENCES

1. Mannervik, B. (1985) The isoenzymes of glutathione transferases, *Adv. Enzymol. Relat. Areas Mol. Biol. 57*, 657−417.
2. Tew, K. D., Monks, A., Barone, L., Rosser, D., Akerman, G., Montali, J. A., Wheatley, J. B., and Schmidt, D. E., Jr. (1996) Glutathione-associated enzymes in the human cell lines of the National Cancer Institute drug screening program, *Mol. Pharmacol. 50*, 149−159.
3. Waxman, D. J. (1990) Glutathione *S*-transferases: role in alkylating agent resistance and possible target for modulation chemotherapy−a review, *Cancer Res. 50*, 6449−6454.
4. Tew, K. D. (1994) Glutathione-associated enzymes in anticancer drug resistance, *Cancer Res. 54*, 4313−4320.
5. Niitsu, Y., Takahashi, Y., Ban, N., Takayama, T., Saito, T., Katahira, T., Umetsu, Y., Nakajima, T., Ohi, M., Kuga, T., Sakamaki, S., Matsunaga, T., Hirayama, Y., Kuroda, H., Homma, H., Kato, J., and Kogawa, K. (1998) A proof of glutathione *S*-transferase π-related multidrug resistance by transfer of antisense gene to cancer cells and sense gene to bone marrow stem cells, *Chem. Biol. Interact. 24*, 325−332.
6. Adler, V., Yin, Z., Fuchs, S. Y., Benezra, M., Rosario, L., Tew, K. D., Pincus, M. R., Sardana, M., Henderson, C. J., Wolf, C. R., Davis, R. J., and Ronai, Z. (1999) Regulation of JNK signaling by GSTp, *EMBO J. 18*, 1321−1334.
7. Ruscoe, J. E., Rosario, L. A., Wang, T., Gate, L., Arifoglu, P., Wolf, C. R., Henderson, C. J., Ronai, Z., and Tew, K. D. (2001) Pharmacologic or genetic manipulation of glutathione *S*-transferase P1-1 (GSTπ) influences cell proliferation pathways, *J. Pharm. Exp. Ther. 298*, 339−345.
8. Lyttle, M. H., Hocker, M. D., Hui, H. C., Caldwell, C. G., Aaron, D. T., Engqvist-Goldstein, A., Flatgaard, J. E., and Bauer, K. E. (1994) Isozyme-specific glutathione *S*-transferase inhibitors: Design and synthesis, *J. Med. Chem. 37*, 189−194.
9. Flatgaard, J. E., Bauer, K. E., and Kauvar, L. M. (1993) Isozyme specificity of novel glutathoine *S*-transferase inhibitors, *Cancer Chemother. Pharmacol. 33*, 63−70.
10. Morgan, A. S., Ciaccio, P. J., Tew, K. D., and Kauvar, L. M. (1996) Isozyme-specific glutathione *S*-transferase inhibitors potentiate drug sensitivity in cultured human tumor cell lines, *Cancer Chemother. Pharmacol. 37*, 363−370.
11. Mammen, M., Chio, S., and Whitesides, G. M. (1998) Polyvalent interactions in biological systems: implications for design and use of multivalent ligands and inhibitors, *Ang. Chem., Int. Ed. 37*, 2754−2794.
12. Rao, J., Lahiri, J., Weis, R. M., and Whitesides, G. M. (2000) Design, synthesis, and characterization of a high-affinity trivalent system derived from vancomycin and L-Lys-D-Ala-D-Ala, *J. Am. Chem. Soc. 122*, 2698−2710.
13. Schaschke, N., Matschiner, G., Zetl, F., Marquardt, U., Bergner, A., Bode, W., Sommerhoff, C. P., and Moroder, L. (2001) Bivalent inhibition of human β-tryptase, *Chem. Biol. 8*, 313−327.
14. Pang, Y.-P., Quiram, P., Jelacic, T., Hong, F., and Brimijoin, S. (1996) Highly potent, selective, and low cost bis-tetrahydroaminacrine inhibitors of acetylcholinesterase, *J. Biol. Chem. 271*, 23646−23649.
15. Parang, K., and Cole, P. A. (2002) Designing bisubstrate analogue inhibitors for protein kinases, *Pharmacol. Ther. 93*, 145−157.
16. Ibarra, C., Nieslanik, B. S., and Atkins, W. M. (2001) Contribution of Aromatic−Aromatic Interactions to the Anomalous pK_a of Tyrosine-9 and the C-Terminal Dynamics of Glutathione *S*-Transferase A1-1, *Biochemistry 40*, 10614−10624.

17. Lyon, R. P., and Atkins, W. M. (2002) Kinetic Characterization of Native and Cysteine 112-Modified Glutathione *S*-Transferase A1-1: Reassessment of Nonsubstrate Ligand Binding, *Biochemistry 41*, 10920−10927.
18. Williams, J. W. and Morrison, J. F. (1979) The kinetics of reversible tight-binding inhibition, *Methods Enzymol. 63*, 437−467.
19. Kuzmič, P., Sideris, S., Cregar, L. M., Elrod, K. C., Rice, K. D., and Janc, J. W. (2000) High-throughput screening of enzyme inhibitors: Automatic determination of tight-binding inhibition constants, *Anal. Biochem. 281*, 62−67.
20. Pace, C. N., Vajdos, F., Fee, L., Grimsley, G., and Gray, T. (1995) How to measure and predict the molar absorption coefficient of a protein, *Protein Sci. 4*, 2411−2423.
21. Oakley, A. J., Lo Bello, M., Ricci, G., Federici, G., and Parker, M. W. (1998) Evidence for an induced-fit mechanism operating in π class glutathione transferases, *Biochemistry 37*, 9912−9917.
22. Cheng, Y., and Prusoff, W. H. (1973) Relationship between the inhibition constant (K_I) and the concentration of inhibitor that causes 50% inhibition (I_{50}) of an enzymatic reaction, *Biochem Pharmacol. 22*, 3099−3108.
23. Sayed, Y., Hornby, J. A., Lopez, M., and Dirr, H. (2002) Thermodynamics of the ligandin function of human class α glutathione transferase A1-1: energetics of organic anion ligand binding, *Biochem. J. 363*, 341−346.
24. Connors, K. A. (1987) *Binding Constants: The Measurement of Molecular Complex Stability*, pp 31−41, Wiley-Interscience, New York.
25. Jencks, W. P. (1987) *Catalysis in Chemistry and Enzymology*, pp 370−375, Dover Publications.
26. Connors, K. A., and Sun, S. (1971) The stability of some molecular complexes in aqueous mixed solvents. Correlation with solvent surface tension, *J. Am. Chem. Soc. 93*, 7239−7244.
27. Oakley, A. J., Lo Bello, M., Nuccetelli, M., Mazzetti, A. P., and Parker, M. W. (1999) The ligandin (nonsubstrate) binding site of human π class glutathione transferase is located in the electrophile binding site (H-site), *J. Mol. Biol. 291*, 913−926.
28. Greco, W. R., and Hakala, M. T. (1979) Evaluation of methods for estimating the dissociation constant of tight binding enzyme inhibitors, *J. Biol. Chem. 254*, 12104−12109.
29. Skoog, D. A., West, D. M., and Holler, F. J. (1990) *Analytical Chemistry*, *5th ed.*, Saunders Publishing, Fort Worth, TX.

BI0346188